

Gamal A. Amhalhel, Piotr Furmański

Institute of Heat Engineering

EXERGY ANALYSIS OF DIFFERENT DESIGN CONCEPTS OF RECEIVERS/REACTORS FOR THERMOCHEMICAL CONVERSION OF CONCENTRATED SOLAR ENERGY

In this paper, exergy analysis of the different design concepts of receivers/reactors utilized for the Thermochemical Energy Conversion process (TCEC) of the concentrated solar energy is presented. The analysis considers all the exergy interactions taking place during the TCEC process. The proposed model has been used to compare the general thermochemical behavior of the three general types of receivers/reactors used for the TCEC process operated in both continuous and discontinuous flow regimes. Comparison of the thermal characteristics of the TCEC process with other Sensible Thermal Energy and Phase Change Thermal Energy Conversion processes has also been presented.

NOMENCLATURE

- A, B, C – the reactant species, A , the product species (B and C)
 a, b, c – stoichiometric coefficient of the reactant species, A , the product species B and C , respectively.
 A – area, m^2
 B – exergy, kJ
 \dot{B} – exergy rate, kJ/s
 \bar{b} – specific molar exergy, $kJ/kmol$
 \bar{b}_f^o – standard specific molar exergy, $kJ/kmol$
 \bar{c}_p – molar specific heat, $kJ/(kmol \cdot K)$
 C – molar concentration, $kmol/m^3$
 CR – solar energy concentration ratio
 E_a – activation energy, $kJ/kmol$
 F – molar flow rate, $kmol/s$
 \bar{h} – specific molar enthalpy, $kJ/kmol$

\bar{h}_f^o	– specific molar enthalpy of formation, kJ/kmol
I	– inert material
k	– frequency factor, 1/s
m	– mass, kg
\dot{m}	– total mass flow rate, kg/s
M	– molecular mass, kg/kmol
p	– pressure, kPa
\bar{R}	– universal gas constant, kJ/(kmol · K)
R/R	– receiver/reactor
S	– entropy, kJ/K
\dot{S}_{gen}	– entropy generation rate, kJ/(s · K)
\bar{s}	– specific molar entropy, kJ/(kmol · K)
\bar{s}_f^o	– specific molar entropy of formation, kJ/(kmol · K)
T	– temperature, K
t	– time, s
t_r	– reference (residence) time, s
y	– mass fraction
V	– volume, m ³
X	– conversion fraction (dimensionless)
$x_{j\theta}$	– the mole fraction of the j -th species at the ultimate dead state

Greek symbols

α	– convective heat transfer coefficient, kW/(m ² ·K)
ϵ	– emissivity
ϕ	– solar flux, kW/m ²
$\rho_{w,R}^{S,L}$	– reflectivity in the short (S) or long (L) wavelength of the thermal radiation spectrum of the receiver/reactor; body (R) or the wall surface (w)
σ	– Stefan-Boltzmann constant, kW/(m ² K ⁴)
τ_w^S	– the transmissivity of the receiver/reactor wall material in the short-wavelength of the radiation spectrum
γ	– porosity of the porous matrix (dimensionless)
ν	– stoichiometric coefficient
Θ	– dimensionless temperature
Ω	– dimensionless time

Superscripts

L	– thermal radiation in long-wave length
*	– unreacted

Subscripts

<i>a</i>	– ambient
<i>c</i>	– cavity
<i>DR</i>	– direct receiver/reactor
<i>e</i>	– outlet
<i>ex</i>	– exchange (e.g. between the <i>R/R</i> wall and the <i>R/R</i> body)
<i>gen</i>	– generation
<i>i</i>	– entering (inlet)
<i>j</i>	– <i>j</i> -th species
<i>o</i>	– dead state
<i>R</i>	– receiver/reactor body
<i>r</i>	– reference flow state condition
<i>S</i>	– surface
<i>w</i>	– receiver/reactor wall

INTRODUCTION

The Thermochemical Energy conversion (TCEC) process provides a means by which the converted thermal energy can be stored as chemical energy in the product species [1, 2, 3]. This has provided several characteristic advantages over the traditional **Sensible** and **Phase Change** TEC processes, for example, the thermal energy can be theoretically stored for an infinite period of time and transported over a long distance, both without the need for insulation [1, 2, 3]. Different types, geometries and configurations of the receivers/reactors were proposed for the TCEC process [1, 2, 3]. The concentrated solar flux impinging on the receiver/reactor wall can also be introduced in different ways depending on the type, geometry and configuration of the receiver/reactor [2]. In general the receivers/reactors can be categorized as: direct volumetric absorption receivers/reactors (i.e. with either a transparent wall (no wall) or a semi-transparent wall) and indirect receivers/reactors (i.e. with an opaque transfer wall). Several base-phase chemical reaction systems (i.e. the phase of the reactant species) have also been proposed for the TCEC process [1, 2].

Amhalhel and Furmanski [3] have performed a comparison assessment of the thermal characteristics of these three general types of receivers/reactors utilizing a zero-order mathematical model, based on first law analysis, of the TCEC process of concentrated solar energy. The first law of thermodynamics considers energy a conservative quantity and consequently, it does not consider the various irreversibilities associated with thermal energy systems [4, 5, 6, 7, 8]. These irreversibilities can be accounted for if an analysis of the thermal systems is developed based on the second law of thermodynamics which addresses the quality of energy – exergy (which is not a conservative quantity). The quality

of energy may be defined as its available portion of energy, e.g., that portion which may be used for producing shaft work [4, 5, 6, 7, 8]. Exergy analysis is necessary in pinpointing quantitatively sources of irreversibility associated with the expenditure of thermal energy in the TCEC process [4, 5, 6, 7, 8]. It also enables the development of an expression for the second law efficiency of the TCEC process of concentrated solar energy [4, 5, 6, 7, 8].

To the authors knowledge the literature lacks preliminary and detailed exergy analysis of the TCEC process. Therefore, it is the objective of the present work to perform a detailed thermodynamic analysis of the TCEC process of concentrated solar energy based on exergy concept. Exergy analysis follows the same path as that of the thermal energy analysis (first law analysis) performed by Amhahel and Furmanski [3] to develop a zero-order mathematical model developed of the TCEC process of concentrated solar energy. Therefore, the exergy analysis accounts for all the exergy interactions taking place during the course of the TCEC process in the receiver/reactor which may have a transparent wall (no wall), semi-transparent or opaque wall. All the exergy destruction terms necessary to define the second law efficiency characterizing the TCEC process will be identified. This will also assist in comparison between the different design concepts of the receivers/reactors operating in both continuous and discontinuous flow regimes. Comparison of the thermal characteristics of the TCEC process with other Sensible and Phase Change TEC processes will also be discussed.

1. THE EXERGY EQUATIONS

The exergy is a thermodynamic function of the system, and for an ideal mixture, the total specific molar exergy \bar{b}_j for the j -th species can be written as [4, 8]:

$$\bar{b}_j = (\bar{h}_j - T_0 \bar{s}_j) - (\bar{h}_{0j} - T_0 \bar{s}_{0j}) \quad (1)$$

where \bar{h}_j and \bar{s}_j are the molar specific enthalpy and the molar specific entropy. The symbols \bar{h}_{0j} and \bar{s}_{0j} stand for the molar specific enthalpy and the molar specific entropy at the restricted dead state condition. **The restricted dead state** is defined as the equilibrium state at the temperature and pressure of T_0 and p_0 , respectively. The temperature T_0 and pressure p_0 at the restricted dead state are constant and usually correspond to the surrounding atmosphere at standard atmospheric conditions, i.e., temperature of $T_0 = 298$ K and a pressure of $p_0 = 101.325$ kN/m² [4, 8]. The total molar enthalpy of the j -th species is defined as [9]:

$$\bar{h}_j = \bar{h}_{jj}^o + \int_{T_r}^T \bar{c}_{pj} dT \quad (2)$$

The total molar entropy of the j -th species \bar{s}_j at the particular temperature and pressure, is usually expressed in terms of the standard molar entropy of formation of the j -th species \bar{s}_{jj}^o at reference temperature, T_r , and pressure, p_r , plus the change in the molar entropy that results when the temperature is raised from reference temperature, T_r , and pressure, p_r , to temperature level, T , and pressure, p . Assuming the ideal mixture it is expressed as [4, 9]:

$$\bar{s}_j = \bar{s}_{jj}^o + \int_{T_r}^T \bar{c}_{pj} \frac{dT}{T} - \theta_j \bar{R} \ln \left(\frac{p}{p_r} \right) - \theta_j \bar{R} \ln x_j \quad (3)$$

For single reactant **solid-based reaction systems** (e.g. the thermal decomposition of the calcium carbonate, CaCO_3 into CaO and CO_2), there is no phase mixing of reactant and products since there is only one product species (CO_2) present in the gaseous phase. Consequently, no gaseous solution is formed. In the case where an inert species, I , is introduced to the thermochemical system then the inert species, I , and the chemical product species which are in the gaseous phase mix and form an ideal solution of perfect gases. For **gas-based reaction systems** e.g. the thermal decomposition of the sulfur trioxide, SO_3 into SO_2 and O_2 , all the chemical species are present in the gaseous phase and as they mix forming the ideal solution of perfect gases. In general, an indicator, θ_j , can be introduced for the j -th species so that:

$$\theta_j = \begin{cases} 1 & \text{for the } j\text{-th species in the gaseous phase} \\ 0 & \text{for the } j\text{-th species in the solid phase} \end{cases} \quad (4)$$

and the corresponding total molar specific entropy at the ultimate dead state condition \bar{s}_{oj} can be written as:

$$\bar{s}_{oj} = \bar{s}_{jj}^o + \int_{T_r}^{T_o} \bar{c}_{pj} \frac{dT}{T} - \theta_j \bar{R} \ln \left(\frac{p_o}{p_r} \right) - \theta_j \bar{R} \ln x_{oj} \quad (5)$$

The ultimate dead state is the equilibrium state that the j -th species will reach with its surrounding at (T_o, p_o, x_{jo}) . The symbols, x_{jo} , denotes the mole fraction of the j -th species at the ultimate dead state. After substituting Eqs (2), (3) and (5) into Eq. (1), the total molar specific exergy of the j -th species, Eq. (1), becomes:

$$\bar{b}_j = \bar{b}_{jj}^o + \int_{T_r}^T \bar{c}_{pj} \left(1 - \frac{T_o}{T} \right) dT + \theta_j \bar{R} T_o \ln \left(\frac{p}{p_r} \right) + \theta_j \bar{R} T_o \ln \left(\frac{x_j}{x_{oj}} \right) \quad (6)$$

By examining Eq. (6), the total specific molar exergy, \bar{b}_j , of the j -th species in the mixture can be divided into **physical exergy** and **exergy due to mixing**. Physical exergy accounts for maximum useful work as the j -th species in the flowing stream reaches the restricted dead state (T_o, p_o) (i.e. the thermal and mechanical equilibrium with its ambient surroundings). The physical exergy is represented by the second and the third terms on the right hand side of Eq. (6). The exergy due to mixing represents the maximum useful work associated with the transition of the j -th species stream from the restricted dead state (T_o, p_o) to the ultimate dead state (T_o, p_o, x_{jo}). This exergy is represented by the last term on the right hand side of Eq. (6). The symbol, \bar{b}_{jj}^o , stands for the chemical exergy at the standard state. The determination of the value of the chemical exergy at the standard state provides a challenging prospective in the exergy analysis of combustion processes (e.g. the chemical exergy of fuels) [10, 11]. However, its value in the case of the TCEC process can be determined utilizing the standard values of thermodynamic functions for the calculation of standard Gibbs free energy [10, 11].

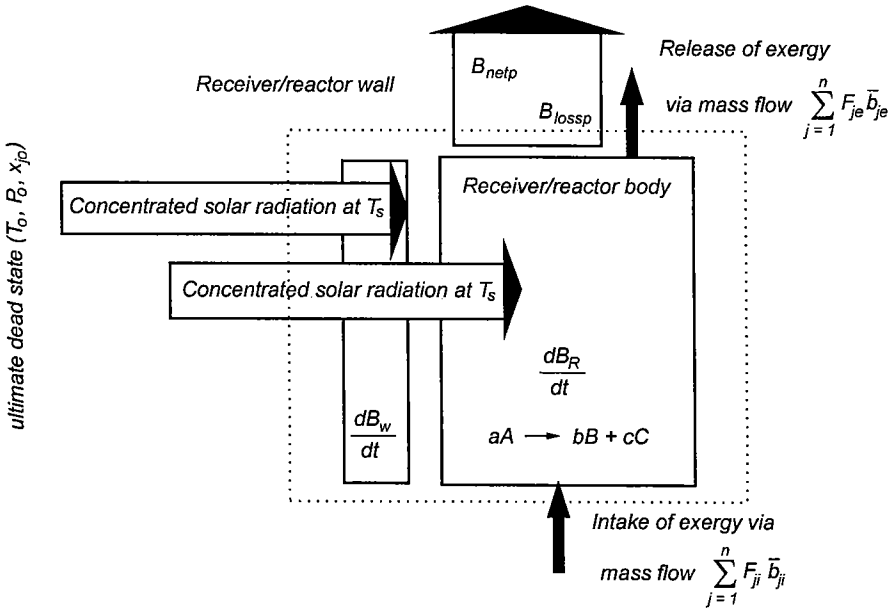


Fig. 1. Exergy interactions for the complete TCEC process

In the following sections the controversy surrounding the expression for entropy and exergy of solar radiation will be addressed. The present analysis considers the more general case of a receiver/reactor having a transparent (no wall), semi-transparent and/or opaque wall (see Fig. 1 in [3]). Most of the governing parameters and consequently the various exergy exchanges that are taking place will be accounted for (Fig. 1). Consequently, there is no need to specify the

particular type of receiver/reactor in advance. The analysis follows the same path as that performed by Amhalhel and Furmanski [3] who have proposed a zero-thermochemical model of the TCEC process based on the first law of thermodynamics. Therefore there is no need to discuss the governing equations describing mass (mole) conservation equations. The exergy analysis considers the more general case of thermal decomposition of a chemical species having the general form of a single reactant, endothermic reversible chemical reaction:



This imposes no restrictions on what type of base-phase reaction system should be considered. Three exergy equations were considered, those of: the receiver/reactor wall, the receiver/reactor body (i.e. **all the species present and accumulated and crossing the boundary of the receiver/reactor**) and the complete TCEC process (i.e. the receiver/reactor wall and the receiver/reactor body). These equations will assist further in identifying total exergy destruction and therefore enabling the definition of the second law efficiency of the TCEC process. The assumptions necessary in developing these exergy equations can be found in [3, 12].

1.1. THE EXERGY EQUATION OF THE RECEIVER/REACTOR WALL

Considerable interest was shown in determining the maximum possible conversion efficiency of solar conversion systems based on second law analysis. This resulted in the development of different expressions for the entropy and the exergy of solar radiation. These expressions were derived from models where solar radiation was considered as a flow of photons [4, 13, 14, 15]. Gribik and Osterle [13] developed a generalized thermodynamic treatment to investigate the controversy surrounding these expressions. Their results showed that these models differed on fundamental grounds based in the nature of the photon gas used to derive the models [13]. Jeter [16] showed that, allowing the idealization that scattering and absorption be excluded, entropy of the direct extraterrestrial radiation is equal to entropy in the initial blackbody state. In doing so, the entropy of the solar radiation was due only to heat flow [16]. Therefore, the maximum efficiency for continuous conversion of extraterritorial radiation to work was given by Carnot engine efficiency [16]. This was consistent with the thermodynamic analysis of the solar energy conversion system which defined the value of the temperature of the high temperature reservoir for the equivalent Carnot cycle having the same solar energy conversion efficiency (i.e., the concept of Carnot cycle equivalence). This temperature may be regarded as the apparent sun temperature which accounts for the special nature of radiation energy together with real dilution of solar radiation. Values of sun equivalent temperature between 5760 K and 6000 K were reported in the literature [15,

16]. In this paper the approximate treatment of exergy of solar radiation, following Jeter's [16] reasoning, will be used.

In the sections to follow, exergy due to thermal radiation in the short-wavelength and long-wavelength range of the spectrum and exergy due to thermal convective heat transfer are considered to accompany the heat flow. The energy exchanged by heat transfer, which is intercepted at temperature of the surrounding, T_a , has a zero exergy value [4, 14].

Recalling Fig. 1 and that the wall material is inert to the chemical reaction taking place in the reactor, the exergy balance for the receiver/reactor wall alone implies that [3]:

$$\begin{aligned}
 V_w \bar{c}_{pw} \left(1 - \frac{T_o}{T_w}\right) \frac{dT_w}{dt} = & \left(\frac{[1 - \tau_w^S - \rho_w^S] + \rho_R^S [\tau_w^S (1 - \tau_w^S) - \rho_w^S (1 - \rho_w^S)]}{(1 - \rho_w^S \rho_w^S)} \right) \times \\
 & \times A_w CR \phi \left(1 - \frac{T_o}{T_s}\right) - \frac{(1 - \rho_R^L) \epsilon_w^L \sigma}{(1 - \rho_w^L \rho_R^L)} A_w (T_w^A - T_R^A) \left(1 - \frac{T_o}{T_R}\right) + \\
 & - \alpha_{ex} A_w (T_w - T_R) \left(1 - \frac{T_o}{T_R}\right) - \dot{B}_{lossw} \quad (8)
 \end{aligned}$$

The term on the left hand side of Eq. (8) gives the rate of change of the non-flow exergy due to the thermal inertia of the R/R wall material. The first term on the right hand side of Eq. (8), represents the exergy increase of the R/R wall as a result of the thermal radiation in the short-wavelength range intercepted by the outer surface of the R/R wall at sun equivalent temperature, T_s . Whereas, the second and third terms represent the exergy decrease of R/R wall as a result of the thermal energy exchanged between the R/R wall and intercepted by the R/R body at the temperature level of the R/R body, T_R . These include thermal radiation exchange in the long-wavelength and thermal convective heat exchange, respectively. The symbol, \dot{B}_{lossw} , stands for the net rate of exergy losses of the R/R wall due to the various irreversible phenomena taking place during the course of the process. The development of the terms appearing in (Eq. (8)) was discussed in more detail in [12].

1.2. THE EXERGY EQUATION OF THE RECEIVER/REACTOR BODY

It is considered that the species are entering the receiver/reactor at the same temperature, T_i , and they are all leaving the receiver/reactor at the same exit temperature, which is the temperature of receiver/reactor body, T_R . It is also assumed that pressure change during the course of operation of the receiver reactor is small compared to the total working pressure and that pressure drop between the inlet and the outlet is small compared to the working pressure and

can be neglected [12]. Other necessary assumptions can be found in [12]. Therefore, recalling Fig. 1 an exergy balance over the receiver/reactor body alone results in [12]:

$$\begin{aligned}
 & \left(\sum_{j=1}^n \gamma V C_j \bar{c}_{pj} \right) \left(1 - \frac{T_o}{T_R} \right) \frac{dT_R}{dt} = \frac{\tau_w^S [1 - \rho_R^S]}{(1 - \rho_w^S \rho_R^S)} A_w CR \phi \left(1 - \frac{T_o}{T_S} \right) + \\
 & + \frac{(1 - \rho_w^L) \varepsilon_R^L \sigma}{(1 - \rho_w^L \rho_R^L)} A_w (T_w^A - T_R^A) \left(1 - \frac{T_o}{T_w} \right) + \alpha_{ex} A_w (T_w - T_R) \left(1 - \frac{T_o}{T_w} \right) + \quad (9) \\
 & - \sum_{j=1}^n v_j (C_A k e^{-E_a/\bar{R}T}) (\gamma V) \bar{b}_j - \sum_{j=1}^n F_{ji} (\bar{b}_j - \bar{b}_{ji}) - \dot{B}_{lossR}
 \end{aligned}$$

The term on the left hand side of Eq. (9) represents the rate of change of the non-flow exergy of the R/R body. The first term on the right hand side of Eq. (9) represents the exergy increase of R/R body as a result of thermal radiation in the short-wavelength range intercepted by the R/R body at sun equivalent temperature, T_S . Whereas, the second and third terms represent the exergy increase of the R/R body as a result of thermal energy exchanged with the R/R wall and intercepted by the R/R body at the temperature level of the R/R wall, T_w . These include thermal radiation exchange in the long-wavelength and thermal convective heat exchange, respectively. The fourth and fifth terms on the right hand side represent the rate of exergy absorbed by the chemical reaction and the net rate of exergy flow across the R/R body. These quantities can be determined by expanding the respective terms appearing in Eq. (9) over all the chemical species involved in the chemical reaction, Eq. (7) and over all the species entering the receiver/reactor. The j -th species which occupy or cross the boundary of the R/R are: the solid matrix, the reactant species, A , the chemical product species (B and C) and the inert species, I . The fifth term on the right hand side of Eq. (9) also includes a thermal energy term which accounts for thermal energy taken by the coolant as it flows across the cooling jacket in the case of the direct volumetric absorption receiver/reactor with no wall i.e. a rotary kiln (see Fig. 3 in [2]). The symbol, \dot{B}_{lossR} , stands for the net rate of the exergy losses of the R/R body due to various irreversible phenomena taking place during the course of the process. The development of the various terms appearing in, Eq. (9), was discussed in a more detail in [12].

1.3. THE EXERGY EQUATION OF THE COMPLETE TCEC PROCESS

An exergy equation for the complete TCEC process can be developed by performing an exergy balance over the whole system of the receiver/reactor wall and the receiver/reactor body (Fig. 1). It can also be obtained by summing the

exergy equations of the receiver/reactor wall and the receiver/reactor body. Using the first approach, the exergy balance over the receiver/reactor wall and the receiver/reactor body implies that [3]:

$$\begin{aligned}
 & V_w \bar{c}_{pw} \left(1 - \frac{T_o}{T_w} \right) \frac{dT_w}{dt} + \left(\sum_{j=1}^n \gamma V C_j \bar{c}_{pj} \right) \left(1 - \frac{T_o}{T_R} \right) \frac{dT_R}{dt} = \\
 & = \left(\frac{[1 - r_w^S - \rho_w^S] + \rho_R^S [\tau_w^S (1 - \tau_w^S) - \rho_w^S (1 - \rho_w^S)]}{(1 - \rho_w^S \rho_w^S)} \right) A_w CR \phi \left(1 - \frac{T_o}{T_S} \right) + \\
 & + \frac{\tau_w^S [1 - \rho_R^S]}{(1 - \rho_w^S \rho_R^S)} A_w CR \phi \left(1 - \frac{T_o}{T_S} \right) - \sum_{j=1}^n v_j (C_A k e^{-E_a/\bar{R}T}) (\gamma V) \bar{b}_j + \\
 & - \sum_{j=1}^n F_{ji} (\bar{b}_j - \bar{b}_{ji}) - \dot{B}_{lossP}
 \end{aligned} \tag{10}$$

The interpretation of the various terms appears in Eq. (10) is the same as those appearing in Eqs. (8) and (9). The symbol, \dot{B}_{lossP} , stands here for the rate of exergy destruction due to various irreversible phenomena taking place during the course of the complete TCEC process [3]. By summing the exergy equation, Eqs. (8) and (9) and comparing the resulting equation with Eq. (10) the exergy destruction of the complete TCEC process can be determined in terms of exergy destruction in the R/R wall and the R/R wall [12]:

$$\begin{aligned}
 \dot{B}_{lossP} = & \left[\left(\frac{(1 - \rho_R^L) \epsilon_w \sigma}{(1 - \rho_w^L \rho_w^L)} A_{ex} (T_w^4 - T_R^4) + \alpha_{ex} A_{ex} (T_w - T_R) \right) \left(\frac{T_o}{T_w} - \frac{T_o}{T_R} \right) + \right. \\
 & \left. + \dot{B}_{lossw} + \dot{B}_{lossR} \right]
 \end{aligned} \tag{11}$$

The exergy destruction terms of the receiver/reactor wall, \dot{B}_{lossw} , and the receiver/reactor body, \dot{B}_{lossR} , can be found from the Gouy-Stodola law [4, 5, 12] and written as:

$$\dot{B}_{lossw} = T_o \dot{S}_{genw} \tag{12}$$

$$\dot{B}_{lossR} = T_o \dot{S}_{genR} \tag{13}$$

The symbols \dot{S}_{genw} and \dot{S}_{genR} denote here the entropy generation of the R/R wall and the R/R body, respectively. According to the Second Law of Thermodynamics these terms should satisfy the following conditions:

$$\dot{S}_{genw} \geq 0 \quad (14)$$

$$\dot{S}_{genR} \geq 0 \quad (15)$$

Entropy generation terms of the receiver/reactor wall and the receiver/reactor body appearing in Eqs. (12) and (13) can be deduced by performing an entropy balance similar to the exergy balance carried out for the above parts of the system. The entropy balance could be performed by utilizing the total molar entropy of the j -th species, \bar{s}_j , Eq. (3), however, this is a tedious task to perform. The alternative approach leading to the exergy equation is to combine the energy and entropy equations [4, 5, 8]. Therefore, the exergy destruction (entropy generation) terms are implicitly included in the exergy equations and appear as terms multiplied by the temperature of the restricted dead state T_o in the exergy equations, Eqs. (8), (9) and (10) [4, 5, 8]. Recalling Eqs. (3), (12) and (13), the entropy generation terms of interest are those due to the total entropy of the j -th species \bar{s}_j , Eq. (3). Furthermore, entropy destruction due to heat transfer that is intercepted by the surrounding at temperature level of, T_a , (Fig. 1) is also included in developing the entropy generation terms. Therefore, upon recalling Fig. 1, Eq. (12) and rearranging Eq. (8) for the entropy generation rate terms in the receiver/reactor wall, **the exergy destruction of the receiver/reactor wall** \dot{B}_{lossw} can be written as [12]:

$$\begin{aligned} \dot{B}_{lossw} = & V_w \bar{c}_{pw} \frac{T_o}{T_w} \frac{dT_w}{dt} + \\ & - \left(\frac{[1 - \tau_w^S - \rho_w^S] + \rho_R^S [\tau_w^S (1 - \tau_w^S) - \rho_w^S (1 - \rho_w^S)]}{(1 - \rho_w^S \rho_R^S)} \right) A_w CR \phi \left(\frac{T_o}{T_S} \right) + \\ & + \varepsilon_w^L \sigma A_w (T_w^A - T_a^A) \left(\frac{T_o}{T_a} \right) + A_w \alpha_w (T_w - T_a) \left(\frac{T_o}{T_a} \right) + \\ & + \frac{(1 - \rho_R^L)}{(1 - \rho_w^L \rho_R^L)} \varepsilon_w^L \sigma A_{ex} (T_w^A - T_R^A) \left(\frac{T_o}{T_R} \right) + A_{ex} \alpha_{ex} (T_w - T_R) \left(\frac{T_o}{T_R} \right) \end{aligned} \quad (16)$$

In a similar manner to Eq. (16), recalling Fig. 1, Eqs. (3), (13) and rearranging Eq. (9) for the entropy generation rate terms of the receiver/reactor body, **the exergy destruction of the receiver/reactor body** \dot{B}_{lossR} is given by [12]:

$$\begin{aligned} \dot{B}_{lossR} = & \left(\sum_{j=1}^n \gamma V C_j \bar{c}_{pj} \right) \frac{T_o}{T_R} \frac{dT_R}{dt} - \frac{\tau_w^S [1 - \rho_R^S]}{(1 - \rho_w^S \rho_R^S)} A_w CR \phi \left(\frac{T_o}{T_S} \right) + \\ & - \frac{(1 - \rho_w^L)}{(1 - \rho_w^L \rho_R^L)} A_{ex} \varepsilon_R^L \sigma (T_w^A - T_R^A) \left(\frac{T_o}{T} \right) + \end{aligned}$$

$$\begin{aligned}
& - \alpha_{ex} A_w (T_w - T_R) \left(\frac{T_o}{T_w} \right) + \sum_{j=1}^n v_j (C_A k e^{-E_a/\bar{R}T}) (\gamma V) T_o \bar{s}_j + \\
& + \sum_{j=1}^n F_{ji} T_o (\bar{s}_j - \bar{s}_{ji}) + [A_{DR_C} \epsilon_{DR_C}^L \sigma (T_R^4 - T_a^4) + A_{DR_S} \epsilon_{DR_S}^L \sigma (T_R^4 - T_a^4) + \\
& + A_{DR_S} \alpha_{DR_S} (T_R - T_a)]_{DR} \left(\frac{T_o}{T_a} \right)
\end{aligned} \tag{17}$$

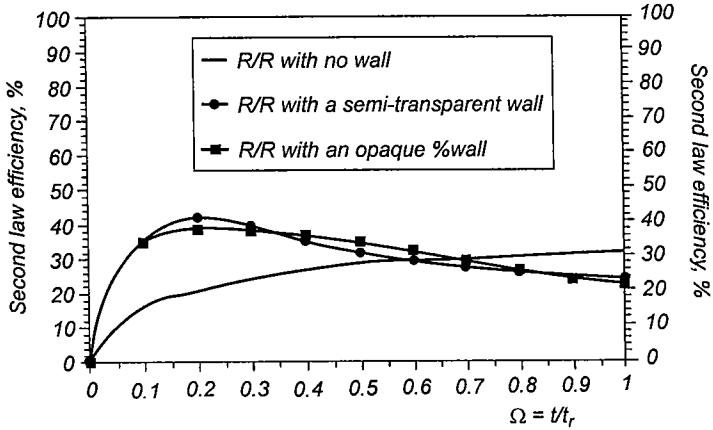


Fig. 2. Variation of the second law efficiency with the dimensionless time for receiver/reactor operating in the discontinuous flow regime

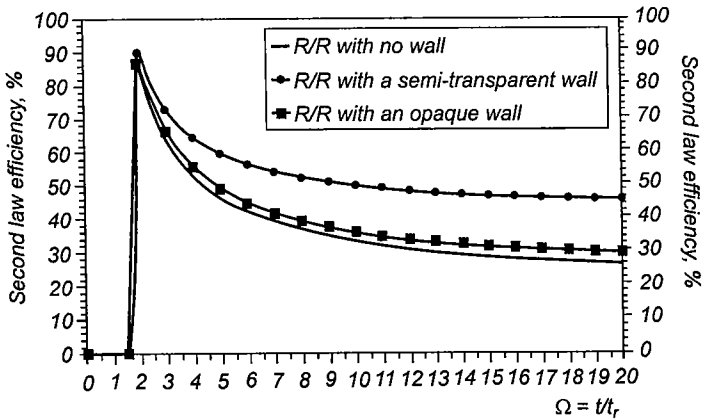


Fig. 3. Variation of the second law efficiency with the dimensionless time for receiver/reactor operating in the continuous flow regime

The last term is added to account for exergy losses in the case of the direct volumetric absorption cavity type receiver/reactor with no wall e.g., the rotary kiln (see Fig. 3 in [2]). Upon substituting Eqs. (16) and (17) into Eq. (11) and rearranging terms, the net rate of exergy destruction (irreversibility) occurring during the course of the complete TCEC process can be written as [12]:

$$\begin{aligned}
 \dot{B}_{lossP} = & - \left[\left(\frac{[1 - \tau_w^S - \rho_w^S] + \rho_R^S [\tau_w^S (1 - \tau_w^S) - \rho_w^S (1 - \rho_w^S)]}{(1 - \rho_w^S \rho_R^S)} \right) \right] + \\
 & + \frac{\tau_w^S [1 - \rho_R^S]}{(1 - \rho_w^S \rho_R^S)} \left[\left(\frac{T_o}{T_s} \right) A_w CR\phi + V_w \bar{c}_{pw} \frac{T_o}{T_w} \frac{dT_w}{dt} + \right. \\
 & + \left(\sum_{j=1}^n \gamma VC_j \bar{c}_{pj} \right) \frac{T_o}{T_R} \frac{dT_R}{dt} + \varepsilon_w^L \sigma A_w (T_w^4 - T_a^4) \left(\frac{T_o}{T_a} \right) + \\
 & + A_w \alpha_w (T_w - T_a) \left(\frac{T_o}{T_a} \right) + \sum_{j=1}^n v_j (C_A k e^{-E_a/\bar{R}T}) (\gamma V) T_o \bar{s}_j + \\
 & + \sum_{j=1}^n F_{ji} T_o (\bar{s}_j - \bar{s}_{ji}) + [A_{DR_c} \varepsilon_{DR_c}^L \sigma (T_R^4 - T_a^4) + A_{DR_s} \varepsilon_{DR_s} \sigma (T_R^4 - T_a^4) + \\
 & + A_{DR_s} \alpha_{DR_s} (T_R - T_a)]_{DR} \left(\frac{T_o}{T_a} \right)
 \end{aligned} \tag{18}$$

2. THE SECOND LAW EFFICIENCY OF THE TCEC PROCESS OF CONCENTRATED SOLAR ENERGY

The exergy equation of the complete TCEC process, Eq. (10), can also be written in the following compact form:

$$\begin{aligned}
 (\dot{B}_{net})_P = & \left[\left(\frac{[1 - \tau_w^S - \rho_w^S] + \rho_R^S [\tau_w^S (1 - \tau_w^S) - \rho_w^S (1 - \rho_w^S)]}{(1 - \rho_w^S \rho_R^S)} \right) \right] + \\
 & + \left(\frac{\tau_w^S [1 - \rho_R^S]}{(1 - \rho_w^S \rho_R^S)} \right) \left[\left(1 - \frac{T_o}{T_s} \right) A_w CR\phi + \dot{B}_{lossP} \right]
 \end{aligned} \tag{19}$$

where the symbol, $(\dot{B}_{net})_P$, represent the net rate of exergy stored during the complete TCEC process and it is given by the sum of the first two terms on the left hand side and the third and fourth terms on the right hand side of Eq. (10).

The second law efficiency of the TCEC process can be defined as the ratio of the net rate of exergy stored during the process to total exergy available for the TCEC process. Upon utilizing this definition and Eq. (19), the second law efficiency of the TCEC process of concentrated solar energy can be written in terms of the entropy generation number, N_G , as [16]:

$$\eta_{II} = 1 - N_G \quad (20)$$

where the entropy generation number is given by [4]:

$$N_G = \frac{\int_0^t \dot{B}_{lossP} dt}{\int_0^t \left[\left(\frac{[1 - \tau_w^s - \rho_w^s] + \rho_R^s [\tau_w^s (1 - \tau_w^s) - \rho_w^s (1 - \rho_w^s)]}{(1 - \rho_w^s \rho_R^s)} \right) + \left(\frac{\tau_w^s [1 - \rho_R^s]}{(1 - \rho_w^s \rho_R^s)} \right) \right] A_w CR \phi \left(1 - \frac{T_o}{T_s} \right) dt} \quad (21)$$

3. COMPARISON BETWEEN THE DIFFERENT DESIGN CONCEPTS OF RECEIVERS/REACTORS OPERATING IN DIFFERENT FLOW REGIMES

The variation over time of both the thermal energy level (i.e. temperature) and the concentrations of the different species leads to variation in the exergy destruction terms appearing in Eq. (10) and in the second law efficiency, Eq. (20). Three types of receiver/reactors are considered for comparison of the TCEC process of the concentrated solar energy each employs the thermal decomposition of calcium carbonate as the reaction system, i.e.



The characteristic design features of each type of receiver/reactor are following:

- a) **Direct volumetric absorption cavity type receiver/reactor (with no wall):**
In this case, the main design features of the receiver/reactor are considered to be the same as those reported by Flamant for the rotary kiln (see Fig. 3 in [2]) [17, 18].
- b) **Direct volumetric absorption receiver/reactor (with a semi-transparent wall):**

In this case, the main design features of the receiver/reactor are considered to be the same as that reported by Flamant [17, 18] for the fluidized bed receiver/reactor with the semi-transparent silica wall (see Fig. 5 in [2]). For continuous flow operation, the TCEC process is assumed to be conducted in the

tubular type receiver/reactor where the flow occurs inside the semi-transparent silica tube. Whereas, for the discontinuous flow regime operation, the TCEC process is assumed to be conducted in the fluidized bed receiver/reactor. This will enable the demonstration of the difference between the TCEC process as conducted in a fluidized bed receiver/reactor and a tubular receiver/reactor.

c) **Indirect receiver/reactor (with an opaque wall):**

In this case the main design features and the type of the receiver/reactor are considered the same as in case b) mentioned above, except that an opaque wall (a steel wall) is utilized.

For **the discontinuous flow operation** the flow conditions are assumed to be similar to those reported by Flamant [18] for the fluidized bed receiver/reactor experiment mentioned above. In this case the reference (**residence**) time ($t_r = 660$ s) is defined as the time for which the TCEC process occurred [16, 18]. However, flow conditions for **the continuous flow operation** are assumed to be similar to those reported by Flamant [18] for the rotary kiln receiver/reactor experiment. The difference being that as soon as a steady state uniform flow condition is reached the solar concentrator is switched on. In this case the mean reference (**residence**) time ($t_r = 91$ s) is defined as the time needed to reach the steady state flow condition [16, 18]. For more detailed information of the value of parameters employed in the analysis the reader should refer to [3, 12]. Moreover, in generating results for thermochemical characteristics of the TCEC process based on second law analysis, it was considered that: the thermal radiation parameters are evaluated on an average basis, the concentrated solar flux is constant; the average value of the sun equivalent temperature is $T_s = 5800$ K, the inert species, I , is considered to be air and it is being treated as a single component gas [12].

For **both operating flow regimes** it was found that, for **the direct volumetric absorption cavity type receiver/reactor with no wall e.g. a rotary kiln**, the total exergy available for the TCEC, corresponding to the denominator of Eq. (21), process was 94.86% of total concentrated solar exergy. This value features the maximum exergy that can be gained from solar radiation. For **the direct volumetric absorption receiver/reactor**, the semi-transparent wall lowers the total exergy available for the TCEC process to the value of 71.91%. However, **the opaque transfer wall**, renders the total exergy available for the TCEC process for the indirect absorption receiver/reactor to the value of 66.40%.

In the following discussion only the thermochemical characteristics as depicted by the second law efficiency will be illustrated (Fig. 3 and Fig. 4). The other main exergy destruction terms which contribute to the entropy generation number were not shown, but were discussed when it was necessary.

For **discontinuous flow operation** (Fig. 3), and for the direct volumetric absorption cavity type receiver/reactor with no wall e.g., the rotary kiln operating in the discontinuous flow regime, it was found that the second law efficien-

cy was $\eta_{II} = 30.89\%$ (i.e. $N_G = 69.11\%$). In this case the coolant contributes about 52% to the entropy generation number. For direct volumetric absorption receiver/reactor with the semi-transparent wall it was found that the second law efficiency was $\eta_{II} = 22.89\%$ (i.e. $N_G = 77.11\%$). Whereas, for the indirect receiver/reactor with an opaque wall, the second law efficiency was $\eta_{II} = 21.30\%$ (i.e. $N_G = 78.70\%$). In this case the main exergy destruction factor which contributed to the entropy generation number was due to the thermal energy exchange of the receiver/reactor wall with the surrounding by both thermal radiation in the long-wavelength range, and thermal convection to about 24% and 11%, respectively.

For **continuous flow operation** (Fig. 4) and for the direct volumetric absorption cavity type receiver/reactor with no wall (e.g., the rotary kiln operating in the continuous flow regime) it was found that, the second law efficiency is $\eta_{II} = 25.78\%$ (i.e. $N_G = 74.22\%$). In this case, the main exergy destruction factor is due to the coolant which contributes about 68% to the entropy generation number. For the direct volumetric absorption receiver/reactor with the semi-transparent wall it was found that the second law efficiency was $\eta_{II} = 44.89\%$ (i.e. $N_G = 55.11\%$). Whereas, for the indirect receiver/reactor with opaque wall, the second law efficiency was $\eta_{II} = 29.04\%$ (i.e. $N_G = 70.96\%$). In this case the main exergy destruction terms which contributed to the entropy generation number were due to the thermal energy exchange of the receiver/reactor wall with the surrounding by both thermal radiation in the long-wavelength range and thermal convection (i.e. to about 30% and 12%, respectively). Whereas, the reactant species, A , and the inert species, I , contributed about 11% and 17% (about 8% is due to mixing), respectively.

For both operating flow regimes, and for the **direct volumetric absorption receiver/reactor with the semi-transparent wall** the main exergy destruction was due to the thermal energy exchange of the receiver/reactor wall with the surrounding by both thermal radiation in the long-wavelength range and thermal convection to the order of 13% and 7.5%, respectively. Consideration of the receiver/reactor operating in the discontinuous flow regime as a fluidized bed resulted in exergy destruction due to the inert species (the fluidized gas) of about 37% (about 17% of this value is due to mixing) higher than that of the continuous flow regime of 17% (about 9% of this value was due to mixing) where the flow of the reactant species occurs inside the tabular receiver/reactor. Finally, consideration of the indirect receiver/reactor operating in the discontinuous flow regime like the fluidized bed resulted in higher exergy destruction due to the inert species (i.e. the fluidized gas) of about 28% (of which about 8% was due to mixing) as compared to that of 17% for the continuous flow regime where the flow of the reactant species was considered as the granular flow through the tabular receiver/reactor.

In general, the receivers/reactors operating in the continuous flow regime showed higher second efficiency than those operated in the discontinuous flow regime. This was due to the fact that receivers/reactors operating in the conti-

nuous flow regime were capable of handling a larger mass of the reactant species than receivers/reactors operating in the discontinuous flow regime. In spite of this result, selection of a particular receiver/reactor for the TCEC process should be based on an economic evaluation of the total cost of the process. For both flow regimes, improvement of the thermochemical characteristics of the direct volumetric absorption cavity type receivers/reactors with no wall requires the suppression of the coolant. The thermochemical characteristics of receivers/reactors with a participating wall can be largely improved by better design that ensures efficient heat transfer between the receiver/reactor wall and the receiver/reactor body. Further improvement is required in controlling thermal energy losses to the surrounding. This latter improvement can easily be achieved through altering the design configuration in such a way that will result in utilizing the cavity effect.

The present results were generated for a particular set of parameters. That is why sensitivity analysis of the influence of the governing parameters will also be valuable in finding the maximum second law efficiency of the TCEC process. Optimization of these parameters is also necessary to determine the optimum operating and designing conditions and consequently, the optimum second law efficiency of TCEC process. An optimization study should also be performed as most of the available literature necessitates economic evaluation of thermal energy systems being assisted by the optimum value of the second law efficiency [4, 5, 6, 7, 8].

3.1. COMPARISON WITH OTHER THERMAL ENERGY CONVERSION (TEC) PROCESSES

Different theoretical and experimental studies of the Sensible and Phase Change TEC (i.e. STEC and PCTEC) processes are available in the literature. They employ different types and configurations of receivers and different thermal energy sources [5, 19, 20, 21, 22, 23, 24]. In these studies the second law (exergy) efficiency is defined as exergy gained by the working fluid during time, t , to the total exergy input during the same time.

The unsteady two-dimensional analysis of the flat-plate **non-concentrating** solar collector for the STEC of solar radiation with time varying insolation was performed by Onyegegbu and Morhenne [19]. Results showed that for a maximum outlet temperature of the working fluid equal to 350 K and for the almost clear day at noon-solar time, the second law efficiency was 5% [19]. An analysis based on exergy analysis alone for the Sensible Thermal Energy storage units showed that, for optimum operating designing conditions, the storage unit was capable of attaining the optimum first and second law efficiencies of $\approx 58\%$ and $\approx 26\%$, respectively [20]. Domanski and Fellah [5] demonstrated that under optimum charging conditions, the Sensible Thermal Energy Storage (STES)

unit, that employed Joulean heaters, would yield the second law efficiencies of 26.63%. Bjurström and Carlsson [21] employed exergy analysis to evaluate both Sensible and Latent Heat Storage units. Their analysis was performed at temperatures $298 \leq T \leq 511$ K that would cover the wide range of transition temperatures of phase change materials. Their analysis revealed that, under optimum operating conditions, both the sensible and latent heat storage units were capable of having the second law efficiencies of 30% [21]. A detailed exergy analysis made by Fellah [22] and based on a lumped system approach and constant, NTU (i.e. Number of Transfer Units) showed that, for moderate flow condition and practical storage size, the second law efficiency for the Sensible and Phase Change Thermal Energy storage units could attain the value of 17% [22]. Whereas, for phase change thermal energy storage units with varying NTU, the results showed second law efficiency from 20% to 30% [22]. Fellah and Domanski [23] studied the performance of a single element at its melting temperature. The influence of the operational and designing parameters on the second law efficiency had also been investigated. Results showed that the storage element destroyed about 70% to 80% of the supplied exergy [23]. Seeking improvement in second law efficiency a study was carried out by Domanski and Fellah [24] for two storage elements in series employing different melting temperatures. The study showed that the second law efficiency can be increased by employing two storage units in series in such a manner that, the up-stream unit had the higher melting temperature [24].

It follows from the above discussion that the second law efficiency of the TCEC efficiency is comparable in magnitude with the STEC and PCTEC processes.

CONCLUSIONS

The present detailed exergy analysis of the TCEC process allowed the following conclusions to be drawn:

- a) In general, receivers/reactors operating in a continuous flow regime showed higher second law efficiency due to their continuous flow operation than those operating in a discontinuous flow regime. The selection of the particular design concept of the receiver/reactor for the TCEC process should be based on an economic evaluation of the total cost of the TCEC process.
- b) Second law efficiency is a measure of entropy generation (i.e., exergy destruction) by the TCEC process. Therefore, it offers the potential to minimize the exergy destruction that will result in minimizing the overall cost of the TCEC process. An economic assessment of the TCEC process should be assisted by the optimization of the governing parameters that would result in optimum second law efficiency.

- c) Regarding the thermal energy level of the TCEC process, its utilization and advantages, the results of the second law efficiency of the TCEC process, carried out for the three general types of receivers/reactor, are comparable in magnitude with the STEC and PCTEC processes.

REFERENCES

- [1] Amhalhel G.A., Furmański P.: Problems of modeling flow and heat transfer in porous media. *Bulletin of Institute of Heat Engineering, Warsaw University of Technology*, **85**, 1997, pp. 55–88.
- [2] Amhalhel G.A., Furmański P.: Theoretical and technical aspects of thermochemical energy conversion of concentrated solar energy. *Bulletin of Institute of Heat Engineering, Warsaw University of Technology*, **89/90**, 2004, pp. 25–58.
- [3] Amhalhel G.A., Furmański P.: Comparison between different design concepts of receivers/reactors for the thermochemical energy conversion of concentrated solar energy. *Bulletin of Institute of Heat Engineering, Warsaw University of Technology*, **89/90**, 2004, pp. 59–83.
- [4] Bejan A.: *Advanced engineering thermodynamics*. John Wiley & Sons Inc. New York 1988.
- [5] Domański R., Giurma Fellah: Exergy as a tool for designing and operating thermal storage systems. *Bulletin of Institute of Heat Engineering, Warsaw University of Technology*, **81**, 1995, pp. 23–45.
- [6] Fellah G.: Exergy analysis for selected thermal energy storage units. Ph. D. Thesis, Warsaw University of Technology, Faculty of Power and Aeronautical Engineering, 1996.
- [7] Said S.A.M., Zubair S.M.: On second law efficiency of solar collectors. *Trans. ASME, J. Solar Energy Eng.*, **115**, 1993, pp. 2–4.
- [8] Szargut J.: International progress in second law analysis. *Energy*, **5**, 1980, pp. 709–718.
- [9] Murr L.A.: *Solar Material Science*. Academic Press, Inc., 1980.
- [10] Szargut J.: Reference level of chemical exergy. *Archives of Thermodynamics*, **9**, 1995, no. 12, pp. 41–52.
- [11] Stepanov V.S.: Chemical energies and exergies of fuels. *Energy*, **20**, 1995, no. 3, pp. 235–242.
- [12] Amhalhel G.A.: Thermodynamic analysis of thermochemical energy conversion of concentrated solar radiation. Ph. D. Thesis, Warsaw University of Technology, Faculty of Power and Aeronautical Engineering, 1998.
- [13] Gribik J.A., Osterle J.F.: The second law efficiency of solar energy conversion. *Trans. ASME, J. of Solar Energy Eng.*, **106**, 1984, pp. 16–21.
- [14] Petela R.: Exergy of heat radiation. *Trans. ASME J., Heat Transfer*, **86**, 1964, pp. 187–192.
- [15] Shafey H.H., Ismail I.M.: Thermodynamics of the conversion of solar radiation. *Trans. ASME, J. of Solar Energy Eng.*, **112**, 1990, pp. 140–144.
- [16] Jeter S.M.: Maximum conversion efficiency for the utilization of direct solar radiation. *Solar Energy*, **26**, 1981, pp. 231–236.
- [17] Flamant G.: Experimental aspects of the thermochemical conversion of solar energy; decarbonation of CaCO_3 . *Solar Energy*, **24**, 1980, pp. 385–395.

- [18] Flamant G.: Thermochimie solaire: Etude de procedes. Application a la decarbonatation de la calcite. These de Docteur Ingenieur, Universite Paul Sabatier Toulouse, 1978.
- [19] Onyegegbu S.O., Morhenne J.: Transient multidimensional second law analysis of time-varying insolation with diffuse component. Solar Energy, **50**, 1993, no. 1, pp. 85–95.
- [20] Domański R., Fellah G.: Thermoeconomic analysis of sensible heat thermal energy storage systems. Applied Thermal Engineering, **18**, 1998, no. 8, pp. 693–704.
- [21] Bjurström H., Bo Carlsson: An exergy analysis of sensible and latent heat storage. Heat Recovery systems, **5**, 1985, no. 3, pp. 233–250.
- [22] Fellah G., Domański R.: Exergy analysis for the optimum performance of phase change thermal storage units. Archives of Thermodynamics, **16**, 1995, pp. 31–47.
- [24] Fellah G., Domański R.: Exergy analysis for the evaluation of a thermal storage system employing PCM's with different melting temperatures. Applied Thermal Engineering, **16**, 1996, pp. 907–919.

ANALIZA EGZERGETYCZNA RÓŻNYCH TYPÓW ODBIORNIKÓW PROMIENIOWANIA/REAKTORÓW DLA TERMOCHEMICZNEJ KONWERSJI ENERGII SKONCENTROWANEGO PROMIENIOWANIA SŁONECZNEGO

Streszczenie

W pracy przedstawiono analizę egzergetyczną różnych typów odbiorników promieniowania/reaktorów chemicznych wykorzystywanych w układach do termochemicznej konwersji energii skoncentrowanego promieniowania słonecznego (TCEC). Analiza uwzględnia wszelkiego rodzaju oddziaływania występujące podczas procesu TCEC. Przy jej pomocy dokonano porównania trzech różnych typów odbiorników promieniowania/reaktorów pracujących zarówno w przypadku przepływu reagentów, jak i jego braku. Przeprowadzono również porównanie sprawności egzergetycznej procesu TCEC z innymi procesami konwersji energii promieniowania słonecznego.